

Negative spin polarization of the $\text{Fe}_3\text{O}_4/\gamma\text{-Al}_2\text{O}_3$ interface measured by spin-resolved photoemission

A. M. Bataille,^{1,*} A. Tagliaferri,² S. Gota,¹ C. de Nadaï,³ J.-B. Moussy,¹ M.-J. Guittet,¹ K. Bouzouane,⁴ F. Petroff,⁴ M. Gautier-Soyer,¹ and N. B. Brookes³

¹DRECAM/SPCSI, CEA Saclay, 91191 Gif-sur-Yvette, France

²INFN, Dipartimento di Fisica del Politecnico, Piazza Leonardo da Vinci 32, 20133 Milano, Italy

³ESRF, Boîte Postale 220, 38043 Grenoble Cedex, France

⁴Unité Mixte de Physique CNRS/Thales, Route Départementale 128, 91767 Palaiseau Cedex, France and Université Paris-Sud, 91405 Orsay, France

(Received 11 August 2005; published 2 May 2006)

We report on spin-resolved photoemission spectroscopy measurements at the interface between a 25-nm-thick Fe_3O_4 (111) thin film and a 2-nm-thick $\gamma\text{-Al}_2\text{O}_3$ (111) layer. The Fe_3O_4 layer remains stoichiometric even after being covered by $\gamma\text{-Al}_2\text{O}_3$ and exhibits a *negative* spin polarization of $\sim -40\%$, after remanence correction. This value should be considered as a lower bound for the spin polarization and demonstrates that Fe_3O_4 remains a spin polarized material even after incorporation in a bilayer.

DOI: [10.1103/PhysRevB.73.172201](https://doi.org/10.1103/PhysRevB.73.172201)

PACS number(s): 75.70.Cn, 75.47.Pq, 72.25.Mk, 79.60.Jv

The discovery of giant magnetoresistance in Fe/Cr multilayers¹ has been followed by a large research effort for almost two decades aiming at developing new materials suitable for spintronics. The interest of a given material is mainly expressed by its spin polarization $P = (N_{\uparrow} - N_{\downarrow}) / (N_{\uparrow} + N_{\downarrow})$, N_{\uparrow} (N_{\downarrow}) standing for majority spin (minority spin) electron density of states at the Fermi level. This property is particularly important for magnetic tunnel junctions (stacks of two magnetic electrodes separated by a thin insulating layer).² Indeed, the tunnel magnetoresistance (TMR), corresponding to the variation of resistance between parallel and antiparallel configurations of the electrode magnetizations, is given in a simple view by the Jullière formula:³ $\text{TMR} = 2P_1P_2 / (1 - P_1P_2)$, P_1 and P_2 being the spin polarizations of the two electrodes. Magnetite (Fe_3O_4) is thus expected to be an interesting electrode material, for band structure calculations predict a half metallic behavior ($P = -100\%$), the conduction being due solely to the minority spin electrons,^{4,5} and it might exhibit high spin polarization at room temperature and above because of its high Curie temperature ($T_C = 860$ K). Despite a large amount of experimental work, there is yet no consensus on the value of the intrinsic spin polarization of Fe_3O_4 , as spin-resolved photoelectron spectroscopy (SR-PES) experiments realized on Fe_3O_4 surfaces reveal a large range of values⁶⁻¹⁰ from -80% to $+16\%$ corresponding to samples grown by different methods and different crystal orientations. Moreover the pertinent parameter for spin dependent tunneling is not the spin polarization of Fe_3O_4 surface, but that of the Fe_3O_4 /tunnel barrier *interface*, the value and sign of which strongly depend on the material used as the tunnel barrier and cannot be guessed from the spin polarization of the Fe_3O_4 surface only.¹¹ The largest TMR results to date with an Fe_3O_4 electrode were obtained on sputtered $\text{Co}/\text{AlO}_x/\text{Fe}_{3-x}\text{O}_4$ trilayers ($+43\%$ at 4 K).¹² Considering an effective spin polarization of $+33\%$ for the $\text{Co}/\text{Al}_2\text{O}_3$ interface,¹³ this leads to a spin polarization of $+53\%$ according to the Jullière formula which is greater than the spin polarization ($+45\%$) reported for metallic Fe using

tunneling experiments.¹⁴ Moreover, these tunneling experiments lead to a *positive* spin polarization at the Fe_3O_4 /alumina interface, while a negative value was reported in most SR-PES experiments⁶⁻⁹ on Fe_3O_4 surfaces and has been predicted by band structure calculations.^{4,5} A direct measurement of the spin polarization at the Fe_3O_4 /alumina interface is therefore clearly needed, and the present paper addresses the unsolved question of the sign of the spin polarization at the Fe_3O_4 /alumina interface.

Direct insight into the spin polarization at the Fe_3O_4 /barrier interface can be gained by using spin-resolved photoelectron spectroscopy (SR-PES),^{15,16} even if the measurement has proven to be difficult and is limited to a few eV around E_F due to the trade-off with signal intensity. To the best of our knowledge, no such experiment has been reported so far concerning Fe_3O_4 covered by a tunnel barrier, and requires a high quality and well-characterized sample. The aim of this paper is to present SR-PES results obtained on a $\text{Fe}_3\text{O}_4/\gamma\text{-Al}_2\text{O}_3$ bilayer epitaxially grown on $\alpha\text{-Al}_2\text{O}_3$ substrates by MBE.

Samples were grown in an MBE setup dedicated to oxide thin films elaboration by co-deposition of atomic oxygen and metal, as described in details elsewhere.¹⁷ High quality Fe_3O_4 (111) thin films can be epitaxially grown onto sapphire (0001),¹⁸ and we also recently developed a method addressing the delicate problem of growing an ultrathin $\gamma\text{-Al}_2\text{O}_3$ (111) crystalline layer on top of a Fe_3O_4 (111) thin film without altering its stoichiometry.¹⁹

The samples were thoroughly characterized prior to the photoemission and x-ray magnetic circular dichroism (XMCD) studies using standard bulk magnetometry [vibrating sample magnetometer (VSM), superconducting quantum interference device (SQUID)] and electrical transport measurements (see Fig. 1). The 25-nm-thick Fe_3O_4 single layer exhibits a rather sharp Verwey transition at 119 K, both when looking at the magnetic or electrical properties of the sample. Bulk single crystals exhibit a first order transition at $T_V = 120$ K, but a broadening has been reported for thin

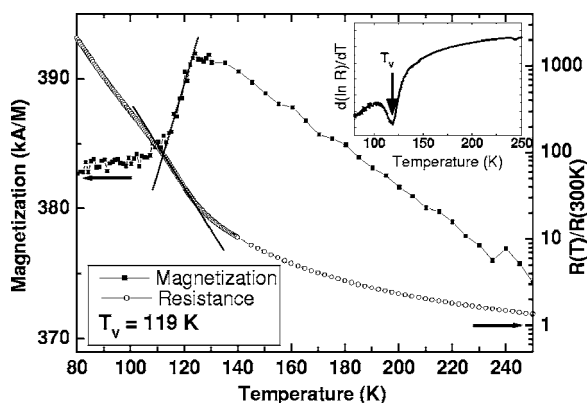


FIG. 1. Verwey transition of the reference Fe_3O_4 sample, observed both in magnetic and transport measurements (straight lines are only guides for the eyes). The inset shows the logarithmic derivative of the resistance in which the local extremum defines the Verwey temperature. The transition occurs at $T_V=119$ K, which is very close to the bulk value.

films.^{20,21} Since any deviation from perfect Fe_3O_4 is known to have a dramatic impact on the Verwey temperature T_V , this sample can genuinely be taken as a stoichiometric Fe_3O_4 reference for XMCD studies of the local magnetism.

The continuity of the Al_2O_3 layer has been monitored locally using conductive tip atomic force microscopy which is a technique extremely sensitive to pinholes given the exponential dependence of electric resistance on the insulator thickness.¹⁹ The measurements (not shown here) demonstrate that the Fe_3O_4 layer is entirely covered by the 2-nm-thick Al_2O_3 layer. This is a crucial requirement for photoemission studies, since the SR-PES signal could be dominated by photoelectrons coming from the Fe_3O_4 surface and not the $\text{Fe}_3\text{O}_4/\gamma\text{-Al}_2\text{O}_3$ interface, in the case of partial coverage.

The room temperature magnetic properties of the $\text{Fe}_3\text{O}_4/\gamma\text{-Al}_2\text{O}_3$ bilayer are shown in Fig. 2. The hysteresis loop is typical of Fe_3O_4 thin films grown in our laboratory: the coercive field is 415 Oe and the remanent magnetization

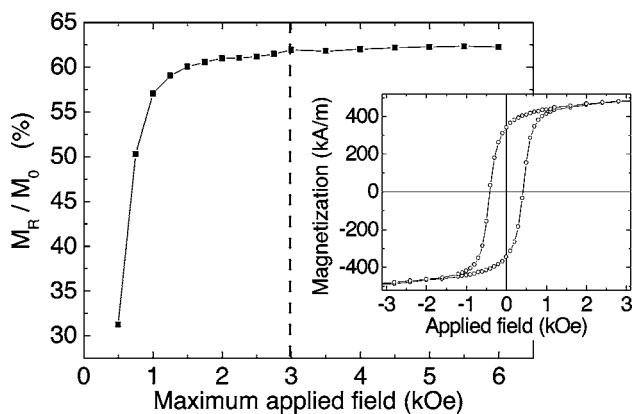


FIG. 2. Remanent magnetization [normalized with respect to $M(20$ kOe)] of the $\text{Fe}_3\text{O}_4/\gamma\text{-Al}_2\text{O}_3$ bilayer as a function of the pulsed field applied by the VSM. The dashed line corresponds to the pulsed field applied during the SR-PES experiments. Inset shows the room temperature hysteresis loop of the $\text{Fe}_3\text{O}_4/\gamma\text{-Al}_2\text{O}_3$ bilayer.

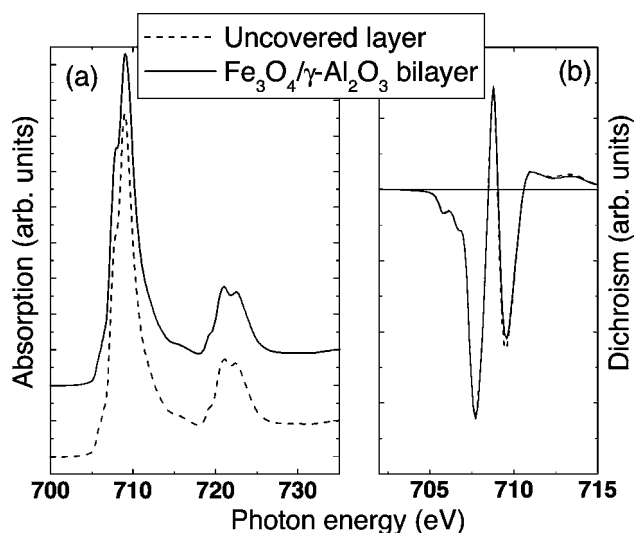


FIG. 3. (a) XAS spectra at the $\text{Fe } L_2$ and L_3 edges of the reference Fe_3O_4 sample (dots) and the $\text{Fe}_3\text{O}_4/\text{Al}_2\text{O}_3$ bilayer (straight line). They have been offset for clarity. (b) XMCD spectra at the $\text{Fe } L_3$ edge (the applied field is 60 kOe). The dichroic signal of the $\text{Fe}_3\text{O}_4/\text{Al}_2\text{O}_3$ bilayer has been multiplied by 1.15 in order to compare the shapes of both spectra.

M_R is 63% of $M(20$ kOe). Since the SR-PES measurements have to be performed in zero applied field, the remanent magnetization of the sample has been checked after sequences emulating the pulsed field applied for the SR-PES experiment: a large positive field was first applied to mimic the one applied for the measurements in the XMCD chamber, then four pulses of a given magnitude H were applied ($-H \rightarrow +H \rightarrow -H \rightarrow +H$) and the remanent magnetization was finally measured. The curve of Fig. 2 demonstrates that a field of 2 kOe is required to reach the remanent magnetization plateau, which is nearly constant for fields larger than 3 kOe.

X-ray absorption spectroscopy (XAS) and x-ray magnetic circular dichroism (XMCD) experiments were performed on the ESRF ID08 beamline using $\sim 100\%$ circularly polarized light both in a dedicated setup using a UHV 60 kOe superconducting magnet and within the SR-PES chamber. The 60 kOe magnetic field was applied making a 30° angle to the film surface so as to reproduce the incident beam/sample/analyzer geometry of the SR-PES chamber. All the magnetic moments are aligned with the external magnetic field H , since the anisotropy field measured by VSM is much lower than the applied field ($H_{\text{an}}=5.5$ kOe for both samples). Figure 3 shows the XAS and XMCD spectra obtained in the XMCD chamber on the reference Fe_3O_4 layer and on the $\text{Fe}_3\text{O}_4/\gamma\text{-Al}_2\text{O}_3$ bilayer. These experiments allow further insight into the magnetic and chemical properties of the samples. In particular, XMCD is known to be extremely sensitive to the Fe valency.²² XAS spectra of the two samples are identical within the experimental uncertainty. Furthermore, the dichroic signal exhibits exactly the same shape as for the free surface showing that the stoichiometry of Fe_3O_4 at the interface has not been affected by subsequent $\gamma\text{-Al}_2\text{O}_3$ deposition. The reasons for the slight loss of amplitude in the case of the bilayer are still to be clarified.

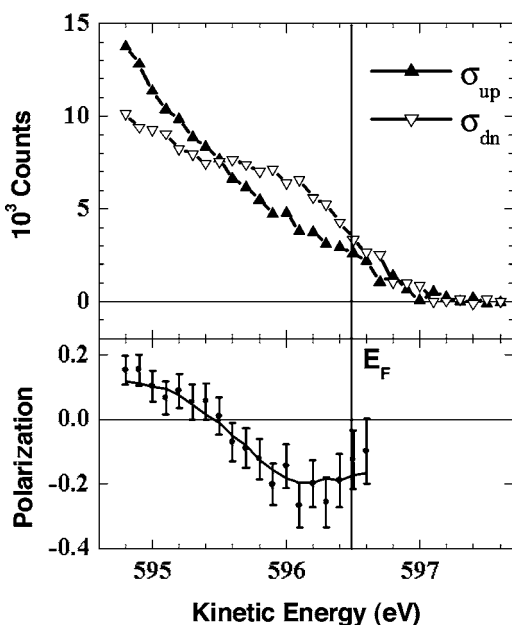


FIG. 4. Spin-resolved photoemission spectra of the valence band of the $\text{Fe}_3\text{O}_4/\gamma\text{-Al}_2\text{O}_3$ bilayer. Upper panel: spin up (\blacktriangle) and spin down (∇) photoemission intensities. Lower panel: spin polarization.

Spin-resolved photoemission was then performed on the bilayer, at normal emission and 30° incidence from the sample normal. No cleaning procedure was performed prior to measurements since the Fe_3O_4 layer was covered by $\gamma\text{-Al}_2\text{O}_3$. This $\gamma\text{-Al}_2\text{O}_3$ layer also weakens the photoemission signal by a factor of ≈ 4 (assuming a mean free path of 1.5 nm for photoelectrons with 600 eV kinetic energy in the 2-nm-thick $\gamma\text{-Al}_2\text{O}_3$ layer). A Mott analyzer was used for spin detection at 20 kV operation voltage. The effective Sherman function of the Mott analyzer has been measured using a reference CuO sample and the value $S_{\text{eff}}=0.14$ was used throughout the whole experiment.^{23,24} The spin detector instrumental asymmetry has been removed by reversing both incident light polarization and sample magnetization, and combining the four resulting sets of data for each individual SR-PES measurement.²⁵ The position of the Fermi level has also been measured using a gold reference sample. The absence of energy shift between spectra taken at different photon beam intensities allows us to exclude sample charging effects during the measurements. The angular acceptance of the analyzer was $\pm 20^\circ$ and the best resolution that could be achieved with good counting rate was 0.7 eV. Such a spectrum took up to 24 h to measure.

The SR-PES result is shown in Fig. 4. At the incident photon energy of 600 eV and with a $\pm 20^\circ$ angular acceptance the measurements can be considered as integrating over the whole Brillouin zone. The spectrum thus gives a good picture of the actual density of states of the sample close to the Fermi level. The spin polarization is found to be $\sim -20\%$ once the energy resolution (0.7 eV) has been accounted for by smoothing the raw data.

This raw value has yet to be corrected since all photoemission measurements have to be performed in zero field after magnetization of the sample by a 3 kOe pulsed mag-

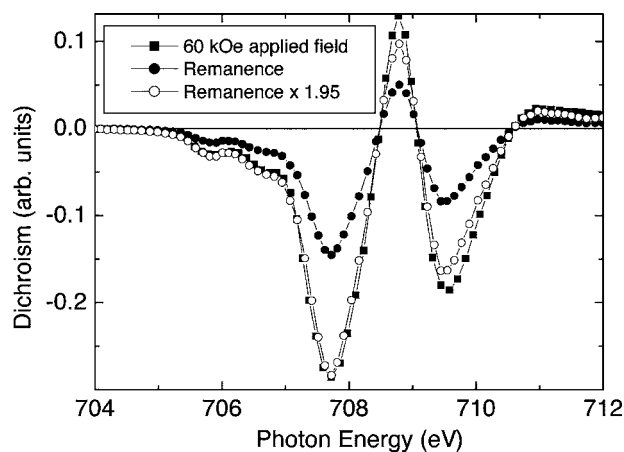


FIG. 5. XMCD spectra of the $\text{Fe}_3\text{O}_4/\gamma\text{-Al}_2\text{O}_3$ bilayer at the Fe L_3 edge. \blacksquare — with a 60 kOe applied field in the XMCD chamber. \bullet — remanence after magnetic pulse, SR-PES chamber. \circ — same as precedent, dichroic signal multiplied by 1.95.

netic field sufficient to reach maximum remanence (see Fig. 2). XMCD spectra were systematically recorded before and after each run of measurement and compared to the dichroic signal recorded in the XMCD chamber under a 60 kOe applied field. As shown by Fig. 5, the $M_R/M(60 \text{ kOe})$ ratio is $\approx 52\%$. Note that this ratio is in fact consistent with the one obtained from VSM measurements, since the remanent magnetization is not normalized by the same “saturation” magnetization [$M(20 \text{ kOe})$ for VSM and $M(60 \text{ kOe})$ for XMCD]. The absence of saturation even in extremely high fields is well-known for magnetite thin films²⁶ and has been attributed to the presence of antiphase boundaries.¹⁷ The raw polarization value from Fig. 4 has to be corrected by a factor of ~ 2 to account for the M_R/M_S ratio.

Taking into account the remanence correction, we obtain a value of -40% for the spin polarization of the $\text{Fe}_3\text{O}_4/\gamma\text{-Al}_2\text{O}_3$ interface. This value is lower than predicted by atomic structure models which lead to $P=-2/3$. However, -40% is only a lower bound value for several reasons. Firstly, the energy resolution of the experiment (0.7 eV) may result in an underestimate of the spin polarization since band structure calculations predict a spin gap of 0.5 eV.²⁷ Moreover, the remanence correction is based on XMCD whose probing depth is rather large compared to XPS. The magnetization at the $\text{Fe}_3\text{O}_4/\gamma\text{-Al}_2\text{O}_3$ interface might therefore be lower than that measured by XMCD. Besides, some contaminants are adsorbed on the surface of the $\gamma\text{-Al}_2\text{O}_3$ layer since no cleaning procedure was performed on the sample. This could give rise to an unpolarized background which lowers the measured spin polarization. Thus the polarization will most probably exceed -40% but this does not allow us to rule out the results of atomic or band structure calculations. The measurement gives nonetheless a *direct* insight on Fe_3O_4 density of states at the electrode barrier *interface*, particularly with respect to the sign of the spin polarization which is found to be *negative* as for the Fe_3O_4 surface. The positive value extracted from tunneling experiments can thus not be ascribed to a change between interface and surface band structures and is related to the tunneling process itself.

In summary, spin-resolved photoemission experiments have been performed on a $\text{Fe}_3\text{O}_4/\gamma\text{-Al}_2\text{O}_3$ epitaxial bilayer in order to measure the spin polarization of Fe_3O_4 at the interface. The sample has been thoroughly characterized by bulk magnetometry in order to establish the minimum magnetic field to be applied in the SR-PES experiment, and by XAS and XMCD in order to check Fe_3O_4 stoichiometry. SR-PES leads to a lower bound of -40% for spin polarization at the $\text{Fe}_3\text{O}_4/\gamma\text{-Al}_2\text{O}_3$ interface after remanence correction.

This experiment clearly gives evidence of a negative spin polarization at the $\text{Fe}_3\text{O}_4/\gamma\text{-Al}_2\text{O}_3$ interface.

We are greatly indebted to the staff of the ESRF and in particular to Peter van der Linden and Kenneth Larsson for designing and realizing the pulsed magnet. We are also indebted to G. Lebras for superconducting quantum interference device measurements, and to F. Sirotti for fruitful discussions.

*Present address: Laboratoire de Physique des Matériaux, Université Henri Poincaré, 54506 Vandoeuvre-les-Nancy, France. Electronic address: alexandre.bataille@lpm.u-nancy.fr

- ¹M. N. Baibich, J. M. Broto, A. Fert, F. Nguyen Van Dau, F. Petroff, P. Etienne, G. Creuzet, A. Friederich, and J. Chazelas, *Phys. Rev. Lett.* **61**, 2472 (1988).
- ²S. A. Wolf, D. D. Aschwalom, R. A. Buhrman, J. M. Daughton, S. Von Molnar, M. L. Roukes, A. Y. Chtchelkanova, and D. M. Treger, *Science* **294**, 1488 (2001).
- ³M. Jullière, *Phys. Lett.* **54A**, 225 (1975).
- ⁴A. Yanase and K. Siratori, *J. Phys. Soc. Jpn.* **52**, 312 (1984).
- ⁵Z. Zhang and S. Satpathy, *Phys. Rev. B* **44**, 13319 (1991).
- ⁶Y. S. Dedkov, U. Rüdiger, and G. Güntherodt, *Phys. Rev. B* **65**, 064417 (2002).
- ⁷M. Fonin, Y. S. Dedkov, J. Mayer, U. Rüdiger, and G. Güntherodt, *Phys. Rev. B* **68**, 045414 (2003).
- ⁸D. J. Huang, C. F. Chang, J. Chen, L. H. Tjeng, A. D. Rata, W. P. Wu, S. C. Chung, H. J. Lin, T. Hibma, and C. T. Chen, *J. Magn. Mater.* **239**, 261 (2002).
- ⁹D. J. Huang, L. H. Tjeng, J. Chen, C. F. Chang, W. P. Wu, A. D. Rata, T. Hibma, S. C. Chung, S.-G. Shyu, C.-C. Wu, and C. T. Chen, *Surf. Rev. Lett.* **9**, 1007 (2002).
- ¹⁰H.-J. Kim, J.-H. Park, and E. Vescovo, *Phys. Rev. B* **61**, 15288 (2000).
- ¹¹J. M. De Teresa, A. Barthélémy, A. Fert, J.-P. Contour, F. Montaigne, and P. Seneor, *Science* **286**, 507 (1999).
- ¹²P. Seneor, A. Fert, J.-L. Maurice, F. Montaigne, F. Petroff, and A. Vaurés, *Appl. Phys. Lett.* **74**, 4017 (1999).
- ¹³F. Montaigne, Ph.D. thesis, Université Paris VII, 1999.
- ¹⁴D. J. Monsma and S. S. P. Parkin, *Appl. Phys. Lett.* **77**, 720 (2000).
- ¹⁵Y. S. Dedkov, M. Fonin, U. Rüdiger, and G. Güntherodt, *Appl. Phys. Lett.* **81**, 2584 (2002).

- ¹⁶M. Sicot, S. Andrieu, P. Turban, Y. Fagot-Revurat, H. Cercellier, A. Tagliaferri, C. De Nadaï, N. B. Brookes, F. Bertran, and F. Fortuna, *Phys. Rev. B* **68**, 184406 (2003).
- ¹⁷J.-B. Moussy, S. Gota, A. Bataille, M.-J. Guittet, M. Gautier-Soyer, F. Delille, B. Dieny, F. Ott, T. D. Doan, P. Warin, P. Bayle-Guillemaud, C. Gatel, and E. Snoeck, *Phys. Rev. B* **70**, 174448 (2004).
- ¹⁸S. Gota, J.-B. Moussy, M. Henriot, M.-J. Guittet, and M. Gautier-Soyer, *Surf. Sci.* **482–485**, 809 (2001).
- ¹⁹A. M. Bataille, J.-B. Moussy, F. Paumier, S. Gota, M.-J. Guittet, M. Gautier-Soyer, P. Warin, P. Bayle-Guillemaud, P. Seneor, K. Bouzehouane, and F. Petroff, *Appl. Phys. Lett.* **86**, 012509 (2005).
- ²⁰S. P. Sena, R. A. Lindley, H. J. Blythe, C. Sauer, M. Al-Kafarji, and G. A. Gehring, *J. Magn. Mater.* **176**, 111 (1997).
- ²¹A. Bollero, M. Ziese, R. Höhne, H. C. Semmelhack, U. Khler, A. Setzer, and P. Esquinazi, *J. Magn. Mater.* **285**, 279 (2004).
- ²²F. Schedin, E. W. Hill, G. van der Laan, and G. Thornton, *J. Appl. Phys.* **96**, 1165 (2004).
- ²³J. Kessler, *Polarized Electrons*, 2nd ed. (Springer-Verlag, Berlin, 1985).
- ²⁴G. Ghiringhelli, K. Larsson, and N. B. Brookes, *Rev. Sci. Instrum.* **70**, 4225 (1999).
- ²⁵T. J. Gay and F. B. Dunning, *Rev. Sci. Instrum.* **63**, 1635 (1992).
- ²⁶D. T. Margulies, F. T. Parker, M. L. Rudee, F. E. Spada, J. N. Chapman, P. R. Aitchison, and A. E. Berkowitz, *Phys. Rev. Lett.* **79**, 5162 (1997).
- ²⁷Z. Zhang, S. Cardoso, P. P. Freitas, X. Batlle, P. Wei, N. Barradas, and J. C. Soares, *J. Appl. Phys.* **89**, 6665 (2001).